Available online at www.sciencedirect.com

ScienceDirect

Polymer 49 (2008) 1604–1610

polymer

www.elsevier.com/locate/polymer

Largely enhanced LED efficiency of carbazole–fluorene–silole copolymers by using TPBI hole blocking layer

Zhitian Liu, Jianhua Zou, Junwu Chen*, Liang Huang, Junbiao Peng, Yong Cao

Institute of Polymer Optoelectronic Materials and Devices, Key Laboratory of Specially Functional Materials of Ministry of Education,
South China University of Technology, Wushan Road, Guangzhou 510640, PR China

Received 3 October 2007; received in revised form 14 January 2008; accepted 20 January 2008
Available online 29 January 2008

Abstract

A new series of soluble 3,6-carbazole–fluorene–silole copolymers (PCz–F–S) with M_w up to 52.1 kDa were synthesized by Suzuki coupling reactions. Chemical structures and optoelectronic properties of the copolymers were characterized by elemental analysis, NMR, UV absorption, cyclic voltammetry, photoluminescence (PL), and electroluminescence (EL) spectra. The main absorption peaks of solutions and films of the copolymers are at 354 nm and 347 nm, respectively, showing the combined contribution from the 3,6-carbazole and fluorene blocks. The silole absorption is at wavelength range between 400 nm and 500 nm. Compared with the solution absorption, largely decreased relative absorption of the silole to the 3,6-carbazole and fluorene blocks can be found for the films of the copolymers. The copolymers possess HOMO levels of around −5.36 eV, mainly from the contribution of 3,6-carbazole. Under excitation, the films of the copolymers show silole-dominated green emissions because of PL excitation energy transfer, with high absolute PL quantum yields up to 86%. EL devices with a configuration of ITO/PEDOT/PCz–F–S/Ba/Al only display a maximum external quantum efficiency of 0.48% whereas a device configuration of ITO/PEDOT/PCz–F–S/TPBI/Ba/Al with TPBI hole blocking layer greatly boosts the efficiency to 3.03% for a practical brightness of 236 cd/m^2. The improved EL efficiency suggests that more balanced charge injection and transport can be realized by inserting the TPBI hole blocking layer.

Keywords: Conjugated polymers; Heteroatom-containing polymers; Light-emitting diodes (LED)

1. Introduction

During the past 30 years, conjugated polymers have drawn much attention. Besides the high conductivity [1], many new properties of conjugated polymers, such as high efficiency in polymeric light-emitting diodes (PLEDs), fast carrier mobility in plastic field effect transistors (FETs), highly efficient power conversion efficiency of plastic solar cells, chemosensing of various targets, etc., have been found [2–8]. For the application of a conjugated polymer as the emissive layer in a PLED [5–8], some important factors, such as higher photoluminescence (PL) efficiency of the polymer, balanced injections of holes and electrons into the emissive layer, and balanced transports and re-combinations of holes and electrons in the emissive layer, play the major roles in the improvement of the PLED efficiency [8–10].

Carbazole is an important building block to construct various conjugated polymers [11–28]. Particularly, poly(3,6-carbazole)s (PCz)s and 3,6-carbazole-based copolymers normally possess HOMO levels between −5.0 eV and −5.4 eV [14–18], which are obviously higher than those of about −5.7 eV for polyfluorenes (PFs) [29–32]. Thus compared with PFs, PCz and 3,6-carbazole-based copolymers can show better hole injections from an ITO or ITO/PEDOT anode [17,33]. Moreover, for PLEDs with PCz or 3,6-carbazole-based copolymers as the emissive layers and further inserting a hole blocking layer with low-lying HOMO levels of around −6.3 eV, an energy barrier of ∼1 eV for hole transporting could be established so that the injected holes may be effectively confined in the emissive layer and the recombination of holes and electrons may only occur in the emissive layer. The device configuration had been

---

* Corresponding author. Tel.: +86 20 8711 4346; fax: +86 20 8711 0606.
E-mail address: psjwchen@scut.edu.cn (J. Chen).

0032-3861/$ - see front matter © 2008 Elsevier Ltd. All rights reserved.
doi:10.1016/j.polymer.2008.01.050

introduced in the evaluation of the blue PLED efficiency with 3,6-carbazole–fluorene copolymers as the emissive layer [14,15].

Recently increasing efforts have been paid to the synthesis and realization of new optoelectronic functionalities of π- or σ-conjugated silole-containing polymers (SCPs) [34–49]. Efficient PLEDs, efficient solar cells (2% energy conversion efficiency), and stable FETs with high hole mobility ($0.06\ \mathrm{cm^2\ V^{-1}\ s^{-1}}$) in air have been demonstrated with the π-conjugated SCPs [44–49]. Though π-conjugated SCPs with alternating copolymer-type structures showed excellent performances in solar cells and FETs [48,49], random copolymer-type SCPs displayed their advantages in PLED applications [17,44–48]. So far, blue PLEDs with maximum external quantum efficiency ($\eta_{\mathrm{EL\ max}}$) of 3.34% have been realized with neat films of random fluorene–3,6-dibenzosilole copolymers as the emissive layer [44], but the $\eta_{\mathrm{EL\ max}}$ of green and red PLEDs based on SCPs is relatively lower [17,45–48]. Green PLEDs with $\eta_{\mathrm{EL\ max}}$ of ∼1.6% were achieved with neat films of SCPs as the emissive layer [45,46] and a higher $\eta_{\mathrm{EL\ max}}$ of 1.99% was realized by using a PF/SCP blending film as the emissive layer [47]. In our previous work, a series of green-emissive silole–fluorene copolymers (PF–S) possessed very high absolute PL quantum yields (Φ_{PL}) up to 87%, but green PLEDs with a neat film of PF–S as the emissive layer in the device configuration of ITO/PEDOT/PF–S/Ba/Al only showed $\eta_{\mathrm{EL\ max}}$ of 0.47% [47]. The low efficiency indicated that the charge injection and transport within the emissive layer were far below the expected balance.

In this work, green-emissive silole units were incorporated in the blue-emissive carbazole–fluorene backbone, affording the green-emissive PCz–F–S copolymers, because of excitation energy transfer process (Scheme 1). The copolymers showed high Φ_{PL} up to 86%. The copolymers possessed HOMO levels of about −5.35 eV because of the contribution of the carbazole building blocks. Since the HOMO level of 1,3,5-tris(*N*-phenylbenzimidizol-2-yl)benzene (TPBI) is −6.2 eV [50], it is expected that effective hole blocking may be achieved in a PLED configuration of ITO/PEDOT/PCz–F–S/TPBI/Ba/Al. Indeed, the hole blocking by the TPBI layer significantly improved the electroluminescence efficiency of PCz–F–S. With PCz–F–S20 as the emissive layer, high $\eta_{\mathrm{EL\ max}}$ of 3.03% and maximum luminous efficiency ($\mathrm{LE_{max}}$) of 7.59 cd/A were achieved, in comparison to $\eta_{\mathrm{EL\ max}}$ of 0.48% and $\mathrm{LE_{max}}$ of 1.20 cd/A for a PLED without the TPBI layer.

2. Experimental

2.1. Instrumentation

^{1}H and ^{13}C NMR spectra were recorded on a Bruker AV 300 spectrometer with tetramethylsilane (TMS) as the internal reference. Molecular weights of the polymers were obtained on a Waters GPC 2410 using a calibration curve of polystyrene standards, with tetrahydrofuran as the eluent. Elemental analyses were performed on a Vario EL elemental analysis instrument (Elementar Co.). UV–vis absorption spectra were recorded on an HP 8453 spectrophotometer. The PL spectra of copolymer solutions and films were obtained on a Jobin Yvon Fluorolog-3 spectrofluorometer. The PL quantum yields of the copolymer films were determined in an Integrating Sphere IS080 (LabSphere) with 405 nm excitation of a He–Cd laser (Melles Griot). EL spectra of the copolymers were recorded on an Instapec IV CCD spectrophotometer (Oriel Co.). Cyclic voltammetry was carried out on a CHI660A electrochemical workstation with platinum electrodes at a scan rate of 50 mV/s against a saturated calomel reference electrode with a nitrogen-saturated solution of 0.1 M tetrabutylammonium hexafluorophosphate ($\mathrm{Bu_4NPF_6}$) in acetonitrile ($\mathrm{CH_3CN}$).

2.2. Synthesis of monomers

Compounds 3,6-bis(4,4,5,5-tetramethyl-1,3,2-dioxaborolan-2-yl)-*N*-hexyl-carbazole (**1**) [17], 2,7-dibromo-9,9-

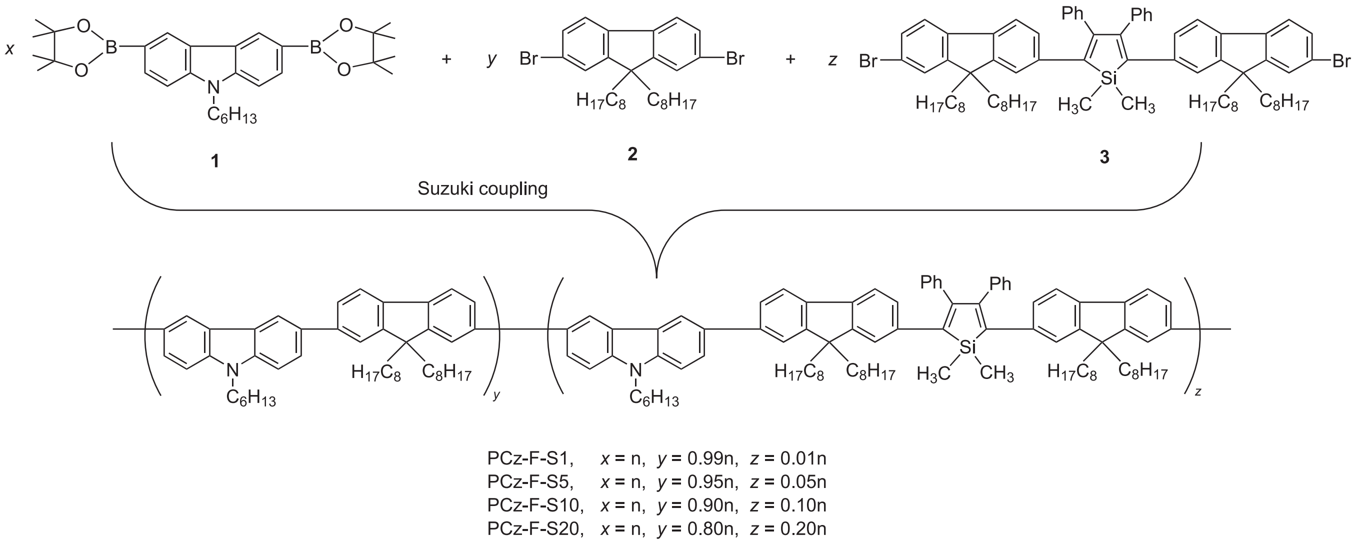

PCz-F-S1, x = n, y = 0.99n, z = 0.01n
PCz-F-S5, x = n, y = 0.95n, z = 0.05n
PCz-F-S10, x = n, y = 0.90n, z = 0.10n
PCz-F-S20, x = n, y = 0.80n, z = 0.20n

Scheme 1. Polymerizations of copolymers PCz–F–S.

dioctylfluorene (**2**) [51], and 1,1-dimethyl-3,4-diphenyl-2,5-bis(9,9-dioctyl-7-bromofluorene-2-yl-)silole (**3**) [47] were prepared according to the literature, and all of them were recrystallized to reach the desirable purity for the next reactions.

2.3. Polymerization

All of the polymerizations were carried out by palladium(0)-catalyzed Suzuki coupling reactions with equivalently molar ratio of the diboronic ester monomer to the dibromo monomers under dry argon protection. A typical procedure for the polymerization of the random copolymer PCz–F–S1 is given below.

Carefully purified 3,6-bis(4,4,5,5-tetramethyl-1,3,2-dioxaborolan-2-yl)-*N*-hexyl-carbazole (**1**) (252 mg, 0.5 mmol), 2,7-dibromo-9,9-dioctylfluorene (**2**) (268 mg, 0.49 mmol), 1,1-dimethyl-3,4-diphenyl-2,5-bis(9,9-dioctyl-7-bromofluorene-2-yl-)silole (**3**) (12 mg, 0.01 mmol), $(PPh_3)_4Pd(0)$ (3.5 mg), and several drops of Aliquat 336 (~150 mg) were dissolved in a mixture of toluene (10 ml) and aqueous 2 M Na_2CO_3 (2 ml). The solution was refluxed with vigorous stirring for 24 h. At the end of polymerization, small amount of **1** (20 mg) was added to remove bromine end groups, and bromobenzene (200 mg) was added as a monofunctional end-capping reagent to remove boronic ester end group. The mixture was then poured into vigorously stirred methanol. The precipitated solid was filtered and washed for 24 h with acetone to remove oligomers and catalyst residues. Light yellow powder of PCz–F–S1 (296 mg) was obtained in 87% yield. Gel permeation chromatography (GPC): M_w 21 200; M_w/M_n 1.9 (Table 1, no. 1). ^1H NMR (300 MHz, $CDCl_3$): δ (TMS, ppm) 8.51 (s, 2H, Ar–*H*), 7.84 (m, 4H, Ar–*H*), 7.75 (m, 4H, Ar–*H*), 7.51 (m, 2H, Ar–*H*), 4.40 (s, 2H, N–C*H*$_2$), 2.14 (s, 4H, C*H*$_2$), 1.96 (s, 2H, C*H*$_2$), 1.42–1.12 (m, 26H, C*H*$_2$), 0.90–0.75 (m, 13H, C*H*$_3$ and C*H*$_2$). Anal. Calcd for: C, 88.44; H, 9.33; N, 2.15. Found: C, 86.80; H, 9.31; N, 2.16.

2.4. PLED fabrication and characterization

The PLEDs were fabricated with configurations of ITO/PEDOT:PSS/emissive layer/Ba/Al and ITO/PEDOT:PSS/emissive layer/TPBI/Ba/Al. Polymers were dissolved in toluene with a concentration of 10 mg/ml and filtered through a 0.45 μm filter. Patterned indium-tin oxide (ITO, ~15 Ω per square)-coated glass substrates were cleaned by routine cleaning procedures, which included sonication in detergent followed by repeated rinsing in distilled water, acetone, and isopropanol, subsequently. After treatment with oxygen plasma, 50 nm of poly(3,4-ethylenedioxythiophene) doped with poly(styrenesulfonic acid) (PEDOT:PSS) (Baytron P 4083, Bayer AG) was spin-coated onto the ITO substrate followed by drying in a vacuum oven at 80 °C for 8 h. A thin film of electroluminescent polymer was coated on the PEDOT:PSS layer by spin-coating inside a nitrogen-filled dry box (Vacuum Atmosphere). The film thickness of the emissive layer was around 80 nm, as measured with an Alfa Step 500 surface profiler (Tencor). For some devices, TPBI with a thickness of 30 nm was evaporated under vacuum to afford the hole blocking layer on the emissive layer. A thin layer of Ba (4–5 nm) and subsequently a 200 nm layer of Al were evaporated under vacuum to construct the cathode. Device performances were measured inside a dry box (Vacuum Atmosphere). Current–voltage (*I*–*V*) characteristics were recorded with a Keithley 236 source meter. The luminance of device was measured with calibrated photodiode. The external quantum efficiency was verified by measuring in the integrating sphere IS080 (LabSphere), and luminance was calibrated by using a PR-705 SpectraScan spectrophotometer (Photo Research) after encapsulation of the devices with UV-curing epoxy and thin cover glass.

Table 1
Molecular weights and elemental analyses of the copolymer

Copolymer	M_w[a]	M_w/M_n[a]	Elemental analysis[b]		
			C	H	N
PCz–F–S1	21 200	1.9	86.80 (88.44)	9.31 (9.33)	2.16 (2.15)
PCz–F–S5	33 400	2.1	86.73 (88.32)	9.24 (9.28)	2.00 (1.99)
PCz–F–S10	46 800	1.7	86.87 (88.21)	9.17 (9.23)	1.81 (1.82)
PCz–F–S20	52 100	2.3	86.49 (88.02)	8.92 (9.15)	1.58 (1.56)

[a] Estimated by GPC in THF on the basis of a polystyrene calibration.
[b] Data given in the parentheses are contents in the feed compositions (leaving groups excluded).

3. Results and discussion

3.1. Polymerization

Random copolymers PCz–F–S were prepared by palladium(0)-catalyzed Suzuki coupling reaction with equivalent molar ratio of the diboronic ester **1** to the dibromo monomers **2** and **3** (Scheme 1). The feed ratios of **1**–**3** were 50:49:1, 50:45:5, 50:40:10, 50:30:20, and the corresponding copolymers are named PCz–F–S1–20 (Scheme 1). All the copolymers are quite soluble in common solvents such as chloroform, toluene, and tetrahydrofuran. The molecular weights of the copolymers are listed in Table 1. The M_w values of the copolymers are between 21.2 kDa and 52.1 kDa with M_w/M_n from 1.7 to 2.3. Along with the increase of the contents of **3** in the feed compositions, the M_w values of the copolymers are elevated, demonstrating the high reactivity of **3**. The elemental analyses of the copolymers are also listed in Table 1. The C, H, and N contents of the copolymers are very close to those of the feed compositions (leaving groups excluded).

3.2. UV absorption and electrochemical properties

Fig. 1A shows the UV–vis absorption spectra of the THF solutions of PCz–F–S1–20. The maxima of the absorption spectra are at ~354 nm. It is well known that the absorptions of PCz and PF are at 310 nm and 380 nm, respectively, thus the absorptions of PCz–F–S1–20 at ~354 nm should be ascribed to the combined contribution from the 3,6-carbazole and fluorene units. A similar absorption of 350 nm was previously reported for a 3,6-carbazole–fluorene alternating copolymer [15]. The results also indicate that the electronic configurations of both the units in the copolymers are almost

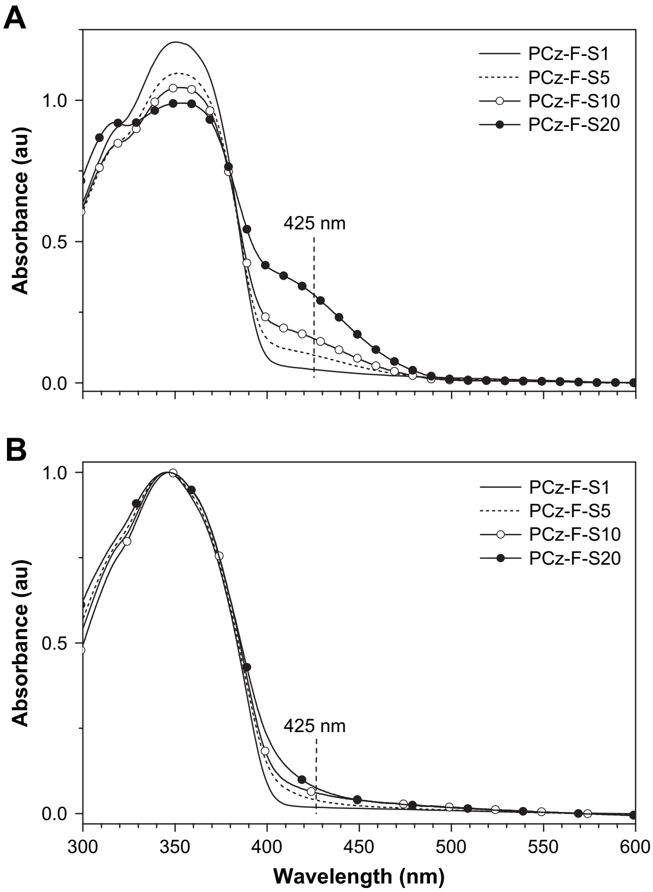

Fig. 1. UV absorption spectra of the copolymers: (A) THF solution (1×10^{-4} M) and (B) thin solid film.

mixed. Along with the increase of silole contents in the four copolymers, the absorptions of the copolymers at ∼354 nm gradually decrease while the absorptions at longer wavelength range between 400 nm and 480 nm increase obviously. Thus the absorptions at the longer wavelength range should be attributed to the contribution of the silole units [46,47]. The results also demonstrate the narrower band gap property of the silole units as compared to the carbazole and fluorene blocks. The absorption edges of the copolymers, obtained from the onset wavelengths of the absorption spectra, are comparable at ∼480 nm. The absorption spectra of the films of the copolymers are shown in Fig. 1B. The maxima of the absorption spectra of the copolymers are comparable at 347 nm, showing 7 nm blue shift and weakened absorptions at ∼315 nm for copolymers with higher silole contents in comparison to those of the solution absorptions. The slightly blue shifting of the film absorption maxima may be attributed to the larger contribution of the carbazole units to the mixed electronic configuration. Similar results were reported before for a carbazole–fluorene alternating copolymer [15]. For PCz–F–S1, the silole absorption almost disappears due to very low silole content in the copolymer. The absorption edge of the absorption spectrum is at 415 nm. For PCz–F–S5, the absorption edge corresponding to the silole absorption is at 480 nm. The absorption edges for PCz–F–S10 and PCz–F–S20 are comparable at 520 nm.

Table 2
Optical band gaps and electrochemical properties of films of the copolymers

Copolymer	Optical band gap[a] (eV)	E_{ox} (V)	HOMO[b] (eV)	LUMO[c] (eV)
PCz–F–S1	2.98	1.00	−5.40	−2.42
PCz–F–S5	2.58	0.92	−5.32	−2.74
PCz–F–S10	2.38	0.93	−5.33	−2.95
PCz–F–S20	2.38	0.98	−5.38	−3.00

[a] Estimated from the onset wavelength of optical absorption of a film.
[b] Calculated according to $\mathrm{HOMO} = -e(E_{ox} + 4.4)$.
[c] Calculated from HOMO level and the optical band gap.

The optical band gaps of the copolymers are listed in Table 2, which are between 2.98 eV and 2.38 eV.

It can be found that the relative absorbance of the silole units to the wide band gap carbazole and fluorene blocks for the film of PCz–F–S as shown in Fig. 1B is obviously lower than that for the solution as shown in Fig. 1A. The absorbance values of PCz–F–S1–20 at an arbitrary wavelength of 425 nm are 0.04, 0.09, 0.15, and 0.32, respectively, as shown in Fig. 1A, but decrease to 0.02, 0.04, 0.06, and 0.08, respectively, as shown in Fig. 1B. Similar phenomena also existed in our previous reports of fluorene–silole copolymers with low silole contents of less than 20% [46,48]. Here we give a preliminary explanation. Polymer chains in films would form strong interactions because of aggregation. Compared with a polymer in a solution, a higher content of the wide band gap blocks such as the coplanar carbazole and fluorene in a copolymer may have advantageous chance to establish face to face stackings in a film. This may supply additional orbitals for electron transitions under an excitation. But the substituted siloles, with non-coplanar chemical structures [52], have lower possibility to form the close stackings in the film, only resulting in very limited additional absorption in the aggregation state.

The electrochemical behaviors of the films of the copolymers were investigated by cyclic voltammetry (CV). The measurement was performed in a 0.1 M n-Bu_4NPF_6 solution in acetonitrile at room temperature. The CV curves were referenced to a saturated calomel electrode (SCE). The ionization potential for HOMO of a conjugated polymer is approximately equal to the onset oxidation potential (vs SCE) plus 4.4 eV (the SCE energy level below the vacuum level) [46–48]. The cyclic voltammograms of the copolymers are shown in Fig. 2. The onsets of oxidation potentials (E_{ox}s) of the copolymers are around 0.96 V (Table 2), from which the calculated HOMO levels of the copolymers are between −5.32 eV and −5.40 eV. The results demonstrate that the HOMO levels of the copolymers are carbazole-dominated. Some reports have found that n-doping process is not reliable to evaluate the LUMO levels of conjugated copolymers and the LUMO level is calculated with the HOMO level and the optical band gap [17,47]. Here the method is also utilized to obtain the LUMO levels of PCz–F–S1–20 and the results are also listed in Table 2. The LUMO levels of the copolymers gradually decrease from −2.42 eV for PCz–F–S1 to −3.00 eV for PCz–F–S20, demonstrating the low-lying LUMO characteristics of the silole units.

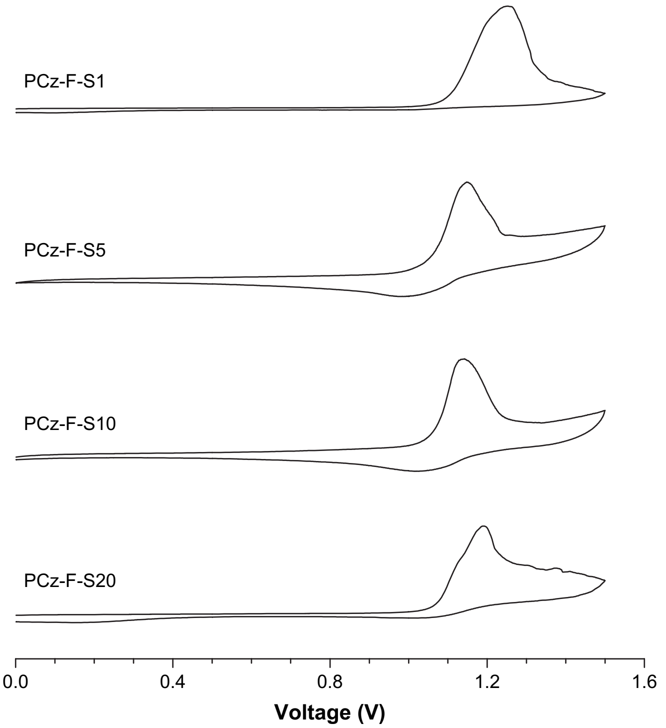

Fig. 2. Cyclic voltammetry of films of the copolymers.

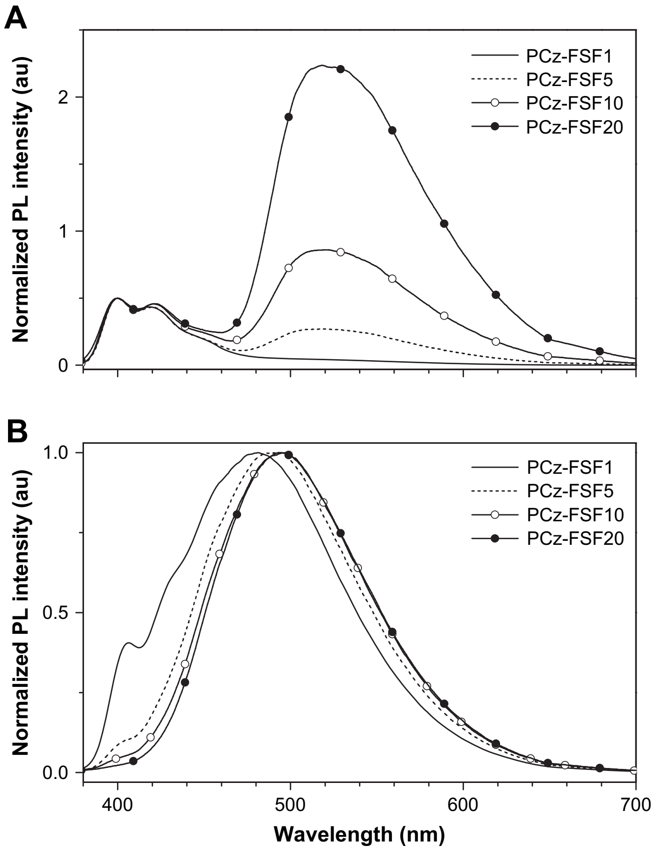

Fig. 3. Photoluminescence spectra of the copolymers: (A) THF solution (4×10^{-5} M) and (B) thin solid film. Excitation wavelength: 360 nm.

3.3. Photoluminescence properties

Photoluminescence spectra of PCz–F–S1–20 in THF solution at a concentration of 4×10^{-5} M are shown in Fig. 3A. The PL peak positions ($\lambda_{\text{PL max}}$) are listed in Table 3. The PL spectrum of PCz–F–S1 exhibits two well-resolved peaks at 400 nm and 419 nm, which had been ascribed to the combined contribution from the carbazole and fluorene blocks with wide band gaps [14], and there is no obvious signature of the silole emission. With the increase of the silole content in the copolymers, new peaks at ∼520 nm, attributed to the silole emission [47], appear in the PL spectra of PCz–F–S5–20. The higher silole content in PCz–F–S5–20 also increases the relative intensity of the silole emission to the two blue-emissive peaks, and the enhanced silole emissions also demonstrate the possibly higher extents of intrachain excitation energy transfer from the wide band gap blocks to the silole units in the copolymers.

Fig. 3B shows the PL spectra of films (80 nm) of PCz–F–S1–20, and the $\lambda_{\text{PL max}}$ values are also listed in Table 3. For PCz–F–S1, the deep blue-emissive band from the carbazole and fluorene blocks is largely weakened and the PL spectrum displays a blue-greenish emission at 481 nm. For copolymer PCz–F–S5–20, the deep blue emissions almost disappear, with gradually red-shifted $\lambda_{\text{PL max}}$ of 491 nm for PCz–F–S5 and 497 nm for both PCz–F–S10 and PCz–F–S20. Compared with the PL spectra of the copolymers in the diluted solutions, the largely enhanced blue-greenish emissions of the films of PCz–F–S1–20 may be mainly attributed to interchain energy transfer established due to the formations of polymer aggregates. It should be noted that the $\lambda_{\text{PL max}}$ values in Fig. 3B for films are slightly blue shifted compared with those in Fig. 3A for the solutions though the absorption spectra in Fig. 1 also show some similar blue shifts. However, fluorene–silole copolymers did not show such differences [47]. Thus the PL blue shifting should be attributed to the influence of 3,6-carbazole units, building blocks with the highest molar ratio in PCz–F–S1–20. In a report by Huang et al., the PL spectrum of a film of poly(3,6-carbazole) displayed a strong shoulder emission at ∼490 nm [18]. The PL spectra of PCz–F–S1–20, as shown in Fig. 3B, may be regarded as mixing emissions from the silole units and the carbazole–fluorene segments. The absolute PL quantum yields (Φ_{PL}) of the films of the copolymers are listed in Table 3. The Φ_{PL} for PCz–F–S1 is 57% and the other three copolymers with higher silole contents can show more efficient PL emissions, with Φ_{PL} values over 80%. The highest Φ_{PL} of 86% for PCz–F–S20 clearly indicates that

Table 3
PL properties of the copolymers[a]

Copolymer	$\lambda_{\text{PL max}}$ (nm)		Φ_{PL}[c] (%)
	Solution[b]	Film	
PCz–F–S1	400, 419	406, 481	57
PCz–F–S5	400, 420, 520	491	80
PCz–F–S10	400, 421, 520	497	83
PCz–F–S20	400, 422, 518	497	86

[a] Excitation wavelength: 360 nm.

[b] In THF (4×10^{-5} M).

[c] Absolute PL quantum yield measured in the integrating sphere; excited by 405 nm He–Cd laser.

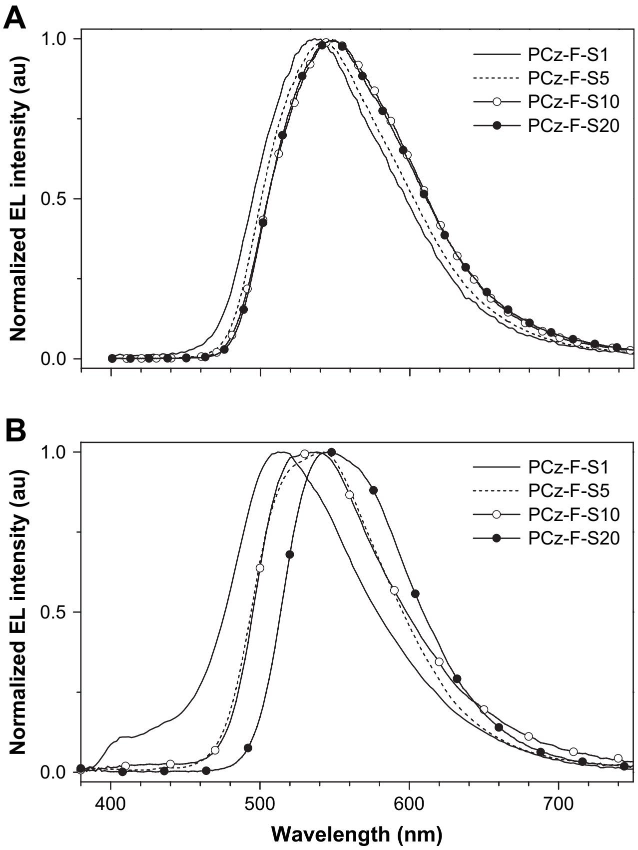

Fig. 4. Electroluminescence spectra of the copolymers with device configurations of (A) ITO/PEDOT/PCz–F–S/Ba/Al (device A) and (B) ITO/PEDOT/PCz–F–S/TPBI/Ba/Al (device B).

siloles, possessing aggregation-induced emission characteristics [35,52], are powerful building blocks to construct conjugated polymers with highly efficient light emission.

3.4. Electroluminescence properties

In order to evaluate the EL properties of the copolymers, EL devices with a traditional configuration of ITO/PEDOT (50 nm)/PCz–F–S (80 nm)/Ba/Al (device A) were fabricated. The EL spectra are shown in Fig. 4A. The four copolymers show the exclusive silole emissions of green lights, demonstrating that the silole units are efficient exciton traps. The peak positions of the EL spectra ($\lambda_{EL\ max}$) are gradually red-shifted from 537 nm for PCz–F–S1 to 548 nm for PCz–F–S20 (Table 4). The EL spectra are also red-shifted relative to the PL emissions of their films. The EL performances of the four copolymers are also listed in Table 4. The $\eta_{EL\ max}$ and LE_{max} for PCz–F–S1 are only 0.07% and 0.17 cd/A, respectively, but a PCz–F–S with a higher silole content can display a better performance. Among the four copolymers, PCz–F–S20 shows the highest $\eta_{EL\ max}$ of 0.48% and LE_{max} of 1.2 cd/A, with a relatively low turn-on voltage of 3.7 V and a maximum brightness (L_{max}) of 4500 cd/m^2.

Since HOMO levels of the copolymers are around −5.36 eV (Table 2), much higher than −6.2 eV for TPBI [50], it is expected that inserting a TPBI layer between PCz–F–S and the cathode would generate effective hole blocking. Thus a PLED configuration of ITO/PEDOT (50 nm)/PCz–F–S (80 nm)/TPBI (30 nm)/Ba/Al (device B) was also utilized. The EL spectra of the devices are shown in Fig. 4B and their $\lambda_{EL\ max}$ values are also listed in Table 4. The $\lambda_{EL\ max}$ for PCz–F–S20 is practically identical to that of the device without the TPBI layer but the $\lambda_{EL\ max}$ values for PCz–F–S1–10 are blue shifted to those of the devices without the TPBI layer. The changing of the EL spectra may be attributed to additional microcavity effect and the changing of exciton generation zone due to the inserting of the TPBI layer. In Fig. 4B, the EL spectra of PCz–F–S5–20 possess more ideal green light bands when compared with that of PCz–F–S1. The EL performances of the devices with the hole blocking layer are also listed in Table 4. The inserting of the TPBI layer slightly elevates the turn-on voltages of the devices. However, the EL efficiencies of the copolymers in device B are all greatly improved. The $\eta_{EL\ max}$ for PCz–F–S1 is 2.71%, showing 38 times increase to that without the TPBI layer. The improving extent for PCz–F–S decreases along with the increase of the silole content in PCz–F–S because of the larger

Table 4
Electroluminescence properties of the copolymers in two device configurations

Device configuration[a]	Emissive layer	V_{on}[b] (V)	$\lambda_{EL\ max}$ (nm)	$\eta_{EL\ max}$[c] (%)	LE_{max}[d] (cd/A)	L_{max}[e] (cd/m^2)
A	PCz–F–S1	6.3	537	0.07	0.17	716
A	PCz–F–S5	4.8	542	0.19	0.48	1011
A	PCz–F–S10	5.8	547	0.32	0.80	1898
A	PCz–F–S20	3.7	548	0.48	1.20	4500
B	PCz–F–S1	7.0	514	2.71	6.78	3203
B	PCz–F–S5	8.0	534	2.66	6.64	3164
B	PCz–F–S10	7.8	534	2.75	6.87	2275
B	PCz–F–S20	5.1	547	3.03	7.59	4923

[a] The active area for all devices is 0.17 cm^2. Device A = ITO/PEDOT (50 nm)/PCz–F–S (80 nm)/Ba/Al; device B = ITO/PEDOT (50 nm)/PCz–F–S (80 nm)/TPBI (30 nm)/Ba/Al.
[b] Turn-on voltage, defined as the voltage needed for brightness of 1 cd/m^2.
[c] Maximum external quantum efficiency.
[d] Maximum luminous efficiency.
[e] Maximum brightness.

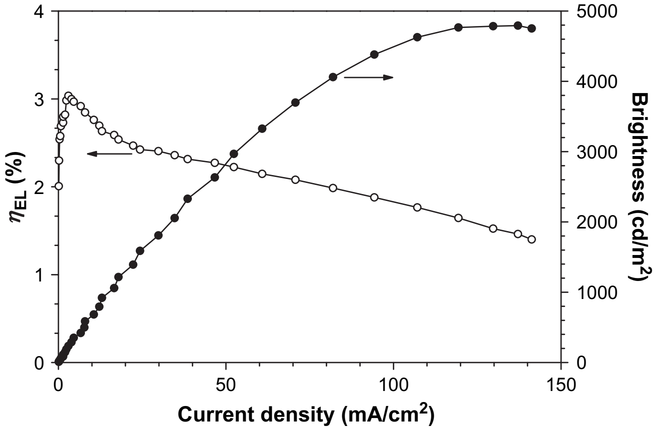

Fig. 5. The external quantum efficiency–current density–brightness characteristics of an EL device with a configuration of ITO/PEDOT/PCz–F–S20/TPBI/Ba/Al.

$\eta_{EL\ max}$ achieved in device A. The L_{max} values of the copolymers in device B are also increased. The improved EL efficiency suggests that more balanced charge injection and transport can be realized in device B. Among the four copolymers in device B, PCz–F–S20 shows the highest $\eta_{EL\ max}$ of 3.03% and LE_{max} of 7.59 cd/A, with a relatively low turn-on voltage of 5.1 V and a high L_{max} of 4923 cd/m^2. The η_{EL}–current density–brightness curves of PCz–F–S20 in device B are shown in Fig. 5 as an example. The device displays the $\eta_{EL\ max}$ of 3.03% for a practical brightness of 236 cd/m^2 at a current density of 3.1 mA/cm^2, and the device can also keep a good η_{EL} of 2.00% for a higher brightness of 4060 cd/m^2 at a current density of 82 mA/cm^2, indicating that SCPs would become the excellent green EL polymers.

4. Conclusions

In this work, green-emissive 3,6-carbazole–fluorene–silole copolymers PCz–F–S1–20 with M_w up to 52.1 kDa, 3,6-carbazole-dominated HOMO levels of around −5.36 eV, and high Φ_{PL} up to 86% were synthesized by Suzuki coupling reactions. Compared with the solution absorption, largely decreased relative absorption of the silole to the 3,6-carbazole and fluorene blocks can be found for the films of the copolymers. The PLEDs with a configuration of ITO/PEDOT/PCz–F–S/Ba/Al only show a low $\eta_{EL\ max}$ of 0.48%. Modified device configuration of ITO/PEDOT/PCz–F–S/TPBI/Ba/Al can boost $\eta_{EL\ max}$ to 3.03% for a practical brightness of 236 cd/m^2, a high efficiency so far reported for green PLEDs with neat films of SCPs as the emissive layer. The largely improved EL efficiency suggests that more balanced charge injection and transport can be realized by inserting the TPBI hole blocking layer.

Acknowledgements

This work was partially supported by National Natural Science Foundation of China (#50773023, #50433030, and #U0634003), Ministry of Science and Technology (#2002CB613404), and Education Ministry of China (Program for NCET-05-0738).

References

[1] Shirakawa H, Louis EJ, MacDiarmid AG, Chiang CK, Heeger AJ. J Chem Soc Chem Commun 1977:578.
[2] Bao Z, Dodabalapur A, Lovinger AJ. Appl Phys Lett 1996;69:4108.
[3] Ma W, Yang C, Gong X, Lee K, Heeger AJ. Adv Funct Mater 2005;15:1617.
[4] Chen L, Mcbranch DW, Wang HL, Helgeson R, Wudl F, Whitten DG. Proc Natl Acad Sci USA 1999;96:12287.
[5] Kraft A, Grimsdale AC, Holmes AB. Angew Chem Int Ed 1998;37:402.
[6] Burroughes JH, Bradley DDC, Brown AR, Marks RN, Mackay K, Friend RH, et al. Nature (London) 1990;347:539.
[7] Akcelrud L. Prog Polym Sci 2003;28:875.
[8] Friend RH, Gymer RW, Holmes AB, Burroughes JH, Marks RN, Taliani C, et al. Nature (London) 1999;397:121.
[9] Forrest SR, Bradley DDC, Thompson ME. Adv Mater 2003;15:1043.
[10] Cao Y, Parker ID, Yu G, Zhang C, Heeger AJ. Nature (London) 1999;397:414.
[11] Morin JF, Leclerc M, Ades D, Siove A. Macromol Rapid Commun 2005;26:761.
[12] Morin JF, Leclerc M. Macromolecules 2001;34:4680.
[13] Boucard V, Ades D, Siove A. Macromolecules 1999;32:4729.
[14] Lu J, Tao Y, D'iorio M, Li Y, Ding J, Day M. Macromolecules 2004;37:2442.
[15] Li Y, Ding J, Day M, Tao Y, Lu J, Diorio M. Chem Mater 2004;16:2165.
[16] Hwang SW, Chen Y. Macromolecules 2002;35:5438.
[17] Wang Y, Hou L, Yang K, Chen J, Wang F, Cao Y. Macromol Chem Phys 2005;206:2190.
[18] Huang J, Niu Y, Yang W, Mo Y, Yuan M, Cao Y. Macromolecules 2002;35:6080.
[19] Iraqi A, Wataru I. Chem Mater 2004;16:442.
[20] Lee J, Lee JI, Sung SJ, Chu HY, Park JK, Shim HK. Macromol Chem Phys 2004;205:2245.
[21] Song SY, Jang MS, Shim HK, Hwang DH, Zyung T. Macromolecules 1999;32:1482.
[22] Meng H, Chen ZK, Liu XL, Lai YH, Chua SJ, Huang W. Phys Chem Chem Phys 1999;1:3123.
[23] Xia C, Advincula RC. Macromolecules 2001;34:5854.
[24] Jenekhe SA, Lu L, Alam MM. Macromolecules 2001;34:7315.
[25] Moon IK, Choi CS, Kim N. Polymer 2007;48:3461.
[26] Qu J, Kawasaki R, Shiotsuki M, Sanda F, Masuda T. Polymer 2007;48:467.
[27] Yang L, Feng JK, Ren AM, Sun JZ. Polymer 2006;47:1397.
[28] Peng Q, Li M, Lu S, Tang X. Macromol Rapid Commun 2007;28:785.
[29] Mei C, Tu G, Zhou Q, Cheng Y, Xie Z, Ma D, et al. Polymer 2006;47:4976.
[30] Liu B, Yu WL, Lai YH, Huang W. Macromolecules 2000;33:8945.
[31] Ma Z, Lu S, Fan QL, Qing CY, Wang YY, Wang P, et al. Polymer 2006;47:7382.
[32] Perzon E, Wang X, Admassie S, Inganas O, Anderson MR. Polymer 2006;47:4261.
[33] Grigalevicius S, Ma L, Qian G, Xie Z, Forster M, Scherf U. Macromol Chem Phys 2007;208:349.
[34] Chen J, Cao Y. Macromol Rapid Commun 2007;28:1714.
[35] Chen J, Xie Z, Lam JWY, Law CCW, Tang BZ. Macromolecules 2003;36:1108.
[36] Chen J, Peng H, Law CCW, Dong Y, Lam JWY, Williams ID, et al. Macromolecules 2003;36:4319.
[37] Sanji T, Sakai T, Kabuto C, Sakurai H. J Am Chem Soc 1998;120:4552.
[38] Yamaguchi S, Goto T, Tamao K. Angew Chem Int Ed 2000;39:1695.
[39] Sohn H, Calhoun RM, Sailor MJ, Trogler WC. Angew Chem Int Ed 2001;40:2104.
[40] Xu C, Yamada H, Wakamiya A, Yamaguchi S, Tamao K. Macromolecules 2004;37:8978.
[41] Chan KL, McKiernan MJ, Towns CR, Holmes AB. J Am Chem Soc 2005;127:7662.
[42] Ohshita J, Hamamoto D, Kimura K, Kunai A. J Organomet Chem 2005;690:3027.
[43] Chen RF, Fan QL, Liu SJ, Zhua R, Pu KY, Huang W. Synth Met 2006;156:1161.
[44] Wang EG, Li C, Mo Y, Zhang Y, Ma G, Shi W, et al. J Mater Chem 2006;16:4133.
[45] Liu MS, Luo J, Jen AKY. Chem Mater 2003;15:3496.
[46] Wang F, Luo J, Chen J, Huang F, Cao Y. Polymer 2005;46:8422.
[47] Liu Z, Wang L, Chen J, Wang F, Ouyang X, Cao Y. J Polym Sci Part A Polym Chem 2007;45:756.
[48] Wang F, Luo J, Yang K, Chen J, Huang F, Cao Y. Macromolecules 2005;38:2253.
[49] Usta H, Lu G, Facchetti A, Marks TJ. J Am Chem Soc 2006;128:9034.
[50] Thomas KRJ, Lin JT, Tao YT, Chuen CH. Chem Mater 2004;16:5437.
[51] Ranger M, Rondeau D, Leclerc M. Macromolecules 1997;30:7686.
[52] Chen J, Law CCW, Lam JWY, Dong Y, Lo SMF, Williams ID, et al. Chem Mater 2003;15:1535.